

Method and Algorithms for Improving Positioning Accuracy for Users with Restricted Signal Bandwidth in 5G NR

Alexander MALTSEV^{a,1}, Igor SERUNIN^b, Andrey PUDEEV^b, Seunggye HWANG^c
and Hyunsoo KO^c

^a*Nizhny Novgorod State University, Nizhny Novgorod, Russia*

^b*LG Electronics Russia R&D Lab, Moscow, Russia*

^c*LG Electronics, Seoul, Korea*

Abstract. In 5G NR systems, users with restricted signal bandwidth may suffer from poor positioning and range performance. In this paper, we present a detailed performance analysis of the frequency hopping method, allowing such users to cover significantly more frequency bandwidth while having a relatively small signal bandwidth in a given time interval. The performance is investigated in a non-stationary frequency selective channel in the absence of phase continuity between hops using coherent or non-coherent joint full frequency bandwidth signal processing algorithms. It was shown that the correct operation of the coherent algorithm requires the phase errors compensation between each pair of signal frequency hops. The proposed non-coherent signal processing algorithm does not require correction of the signal phases and demonstrates its advantages for high mobility users in comparison with the coherent algorithm.

Keywords. 5G NR, frequency hopping, coherent and non-coherent combining, phase error compensation, Doppler effect.

1. Introduction

Positioning in 5G NR was first introduced in Rel-160 and in the next Rel-17[2], it received a significant improvement. Improvements include improving accuracy, reducing positioning delay and UE power consumption. The implemented methods and algorithms in Rel-17 made it possible to achieve positioning accuracy of several tens of centimeters for certain scenarios. The description of algorithms for improving the positioning is presented in [3][4][5]. One of the main parameters for determining the positioning is the frequency bandwidth of the reference signals for determining the locations of UEs. The reference signals for positioning are the position reference signals (PRSs) and the sounding reference signals (SRSs) for the DL (Downlink) and Uplink (UL), respectively. The bandwidths of these reference signals are 100 MHz and 400 MHz for FR1 and FR2 respectively (Frequency range FR1 is from 450 to 6000 MHz and Frequency range FR2 is from 24250 to 52600 MHz). However, the restricted signal bandwidth UEs, often called the reduced capability UEs (RedCap UEs), have a

¹Alexander Maltsev is the corresponding author, e-mail: maltsev@rf.unn.ru. This work was partially supported by the Advanced School of Engineering of the Nizhny Novgorod State University.

significantly lower total signal bandwidth (20 MHz or less). Therefore, the accuracy of location measurement performed for the RedCap UEs will be significantly less in comparison with the standard 5G NR UEs.

One possible solution to the bandwidth restricted UE problem is to use the frequency hopping method. This method was widely discussed at 3GPP TSG RAN1 (3rd Generation Partnership Project Technical Specification Group Radio Access Network) meetings #110 - #114 as the best way to solve the RedCap UE's signal small bandwidth problem. The method is based on the observation by the receiver of signals with a restricted bandwidth, obtained using frequency hopping measurements, with their subsequent combination into the implementation of one wideband signal. For this method to work correctly, it is necessary that the narrowband reference signals in adjacent frequency bands provide a consistent combination of them into one wideband signal.

The main purpose of this paper is to present a detailed performance analysis of the frequency hopping method for various mobility scenarios using the super-resolution Multiple Signal Classification (MUSIC) Time Difference of Arrival (TDoA) estimation algorithm. The analysis is based on the results obtained using the developed System Level Simulator (SLS) for positioning. It is revealed that the coherent algorithm of joint processing of hops has a disadvantage, which consists in the requirement of the narrowband reference signal phases adjustment between all hops for its proper operation. At the same time, the performance of the proposed simple method of non-coherent joint processing of hops does not depend on phase errors of the narrowband reference signals and has its advantage over the coherent algorithm in the case of high UE mobility.

2. Algorithms for improving positioning accuracy

2.1. Using the super-resolution MUSIC algorithm

The super-resolution MUSIC algorithm is a so-called super-resolution harmonic analysis algorithm that is typically used for frequency and direction estimation. It can also be applied for the time of arrival estimation, as is shown in a number of papers [6][7][8]. For using this algorithm in time domain, it is necessary to estimate the correlation matrix in the frequency domain. It is assumed that we know the demodulated reference signals value on each subcarrier, which is equivalent to the simplest least squares (LS) estimation of the channel transfer function. The idea of a coherent algorithm is to stitch demodulated reference signals transmitted in different frequency bands into one wideband signal and evaluate one correlation matrix for it. On the contrary, in a non-coherent algorithm, its own correlation matrix is evaluated for each demodulated narrowband reference signal (hop), and then these matrices are averaged for joint processing.

To improve the single estimation of correlation matrix, it may be averaged over all observation periods (bands), with the shift by one subcarrier. It is necessary to choose the optimal ratio between the size of the correlation matrix and the number of averaging operations. The estimated correlation matrices for a coherent and non-coherent algorithm can be written as follows (Eq.(1)):

$$\begin{aligned}
R_{xx}^1 &= \frac{1}{N_1 - L_1 + 1} \sum_{k_1=0}^{N_1-L_1} \mathbf{X}_1(k_1) \mathbf{X}_1(k_1)^H, \\
R_{xx}^2 &= \frac{1}{N^{hop}} \sum_{m=0}^{N^{hop}-1} \left(\frac{1}{N_2 - L_2 + 1} \sum_{k_2=0}^{N_2-L_2} \mathbf{X}_2^m(k_2) \mathbf{X}_2^m(k_2)^H \right), \\
\mathbf{X}_1(k_1) &= [x(k_1) \dots x(k_1 + L_1 - 1)]^T, \\
\mathbf{X}_2^m(k_2) &= [x(k_2) \dots x(k_2 + L_2 - 1)]^T,
\end{aligned} \tag{1}$$

where R_{xx}^1 and R_{xx}^2 are the estimated correlation matrices for coherent/non-coherent algorithms, \mathbf{X}_1 are the stitched demodulated reference signals from all the hops by length N_1 , \mathbf{X}_2^m are the demodulated reference signals from the m -th hop by length N_2 , m are the hop indices in the configuration, N^{hop} is the number of hops in the configuration, L_1 is the size of the estimated correlation matrix from all the stitched hops for the coherent algorithm, L_2 is the size of the estimated correlation matrix from one hop for the non-coherent algorithm. We will call the forward smoothed correlation matrices the estimates of the correlation matrices R_{xx}^1 and R_{xx}^2 . We can improve the estimates of the correlation matrices using forward-backward correlation matrices as follows (Eq.(2)):

$$\begin{aligned}
R_{xx}^{1(FB)} &= \frac{1}{2} (R_{xx}^1 + R_{xx}^{1(B)}), \\
R_{xx}^{2(FB)} &= \frac{1}{2} (R_{xx}^2 + R_{xx}^{2(B)}),
\end{aligned} \tag{2}$$

where $R_{xx}^{1(FB)}$ and $R_{xx}^{2(FB)}$ are the forward-backward smoothed correlation matrices for coherent/non-coherent algorithms, $R_{xx}^{1(B)}$ and $R_{xx}^{2(B)}$ are the backward smoothed correlation matrices for coherent/non-coherent algorithms. It can be obtained by flipping over the anti-diagonal and transposing. Forward-backward smoothing in most cases gives some gain. It allows achieving the minimum positioning error for some ratio between the smoothing window size and the total number of available samples.

Although the average over a larger bandwidth may increase the accuracy, we should note that the estimates under the sums (1) are not independent due to channel coherence. The major gain may come with averaging over several receive antennas or over independent time instants.

With the fixed total number of demodulated reference signals, different correlation matrix sizes can be selected, leaving more or less opportunities for averaging. For the smaller matrix size, the averaging can be large, and we can get accurate matrix estimation, although due to size it cannot properly represent channel statistic and the final positioning accuracy can be low. On the contrary, selection of the larger matrix size will leave no space for averaging and again, final accuracy may be decreased due to inaccurate correlation matrices estimation for both considered algorithms.

The analysis made by simulations shows that the value of the coefficient of the size of the smoothing window, which is close to the optimal value, is about 0.5-0.6 of the total number of available samples. This means that for each bandwidth size, the size of the correlation matrix should be about half of the total number of demodulated reference signals.

The next parameter that needs to be determined for correct application of the MUSIC algorithm is the number of the channel multipath components L_p using the

minimum description length (MDL) criterion, described in [7]. The distance between transmitter (TX) and receiver (RX) can be determined by finding the time delays at which the following MUSIC pseudo-spectrum achieves maximum values as follows (Eq.(3)):

$$\begin{aligned}
 \tau_{grid} &= \left[0\Delta d \frac{c}{f_s}, 2\Delta d \frac{c}{f_s}, \dots, M\Delta d \frac{c}{f_s} \right]^T, \\
 \mathbf{V}^1 &= \left[1, e^{j2\pi\tau_{grid}\Delta f}, \dots, e^{j2\pi\tau_{grid}\Delta f(L_1-1)} \right], \\
 \mathbf{V}^2 &= \left[1, e^{j2\pi\tau_{grid}\Delta f}, \dots, e^{j2\pi\tau_{grid}\Delta f(L_2-1)} \right], \\
 S_{MUSIC}^1 &= \frac{1}{\sum_{k=L_p^1}^{L_1-1} |\mathbf{V}_k^1 \mathbf{Q}_n^1|^2}, \\
 S_{MUSIC}^2 &= \frac{1}{\sum_{k=L_p^2}^{L_2-1} |\mathbf{V}_k^2 \mathbf{Q}_n^2|^2},
 \end{aligned} \tag{3}$$

where S_{MUSIC}^1 and S_{MUSIC}^2 are MUSIC pseudo-spectra for coherent/non-coherent algorithms, L_p^1 and L_p^2 is the estimated number of multipath components for coherent/non-coherent algorithms, \mathbf{V}^1 and \mathbf{V}^2 are delay steering matrices for coherent/non-coherent algorithms, \mathbf{Q}_n^1 and \mathbf{Q}_n^2 are matrices of eigenvalues corresponding to the noise eigenvalue (sizes $L_1 \times (L_1 - L_p^1)$ and $L_2 \times (L_2 - L_p^2)$, accordingly), Δf is subcarrier spacing, f_s is the sample rate, Δd is the search step, τ_{grid} is time grid with a step Δd to find the maximum, $M\Delta d$ is the search length.

Modified TDoA Chan algorithm with selection of several AP subsets and weighting based on residuals is used for absolute position estimation. Algorithms for determining absolute positioning are described in detail in [9][10][11].

2.2. The algorithm for adjusting the phase error between hops

For a UE with a restricted signal bandwidth, when switching between frequencies, it may be necessary to change its output Radiofrequency (RF) circuits, and thus phase continuity between hops may not be established. This problem is one of the disadvantages of the proposed method when using a coherent algorithm. In this regard, the application of a coherent algorithm requires phase alignment between each pair of hops to eliminate phase errors. This procedure can be performed by overlapping the frequency part for neighboring hops to estimate and compensate the phase error. Thus, the estimation of the phase error for one of the pairs of hops $\widehat{\varphi}_{21}$ in the configuration can be made as follows (Eq.(4)):

$$\widehat{\varphi}_{21} = E\{arg\{Y_1 Y_2^*\}\}, \tag{4}$$

where Y_1, Y_2 the areas of overlapping of are demodulated received reference signals (hops) for the first and second hops in the configuration, arg is the argument of a complex number, E is the averaging. After the evaluation of the phase error between a pair of hops, the phase of the second hop is aligned relative to the first one as follows (Eq.(5)):

$$\mathbf{X}_2^{adjust} = \mathbf{X}_2 e^{-j\widehat{\varphi}_{21}}, \tag{5}$$

where X_2 and X_2^{adjust} are demodulated received reference signals (hops) for the second hop before and after adjusting the phase error, respectively. This procedure is performed for each pair of neighboring hops in the configuration successively until full

phase continuity is achieved. This algorithm is based on the standard algorithm used in orthogonal-frequency-division-multiplexing (OFDM) systems for carrier frequency offset (CFO) compensation, as described in [12][13][14].

3. Simulation assumptions for estimating positioning accuracy

The main parameters of the scenario used for estimating positioning accuracy are shown in Table 1. The Indoor Factory with Sparse clutter and High base station height (InF-SH) scenario of 5G NR network deployment described in 3GPP TR 38.901[15] is used to evaluate the UE's positioning accuracy in the developed SLS. This scenario represents large factory halls with sparse clutters, which are large machines made up of regular metal surfaces. In this scenario, the transmission and reception points (TRPs) are placed in a rectangular room, 300m x150m in size, and the UE can occupy any position with equal probability. The number of TRPs is 18 and the distance between them is 50m. The well-known 3GPP-adopted channel model [15] that thoroughly takes into account path losses, shadowing, fast fading, Doppler and antenna effects is used for simulations.

Table 1. Main scenario parameters for estimating positioning accuracy.

Parameters	Assumption
Carrier Frequency	3.5 GHz
Transmission Bandwidth	86.4 MHz (240 RBs)
Scenario	InF-SH
SCS	30 kHz
Type of reference signal	UL SRS, Comb 4
Frequency hopping pattern configuration	17.3 MHz (48RBs) x 5 slots Diagonal hop pattern
Size of reference signals	1 hop: 576 subcarriers 5 hops: 2880 subcarriers
Coefficient of the size of the smoothing window	0.6
TX/RX Antenna configuration	1x1
Deployment	Total number of UEs = 500 UE's vehicle speed = 3 km/h; 30 km/h; 60 km/h; 120 km/h Room size, m: length = 300 width = 150 height = 25
Algorithms of joint processing hops	Coherent/Non-coherent
Distance algorithm	MUSIC
Positioning algorithm	TDoA (Chan)
Phase between hops	Uniform random, $(0, 2\pi)$

The reference signals are UL SRS, the configurations of which are described in the 3GPP technical specification[16]. In the current Rel-18 specification, UL SRS configurations may not support all required combinations of hop count and occupied bandwidth. So, for the considered 5-hop configuration, the maximum achievable bandwidth is only 86.4 MHz, where one hop occupies 17.3 MHz bandwidth. For this reason, this particular configuration was used in this work for simulations.

Figure 1 shows an illustration of the allocation of 5 hops with and without overlaps. The SRS has a comb structure and can occupy several OFDM symbols in a slot, depending on the selected configuration, but when folding the sequence from each OFDM symbol of the slot, the SRS signal covers the entire band of one hop.

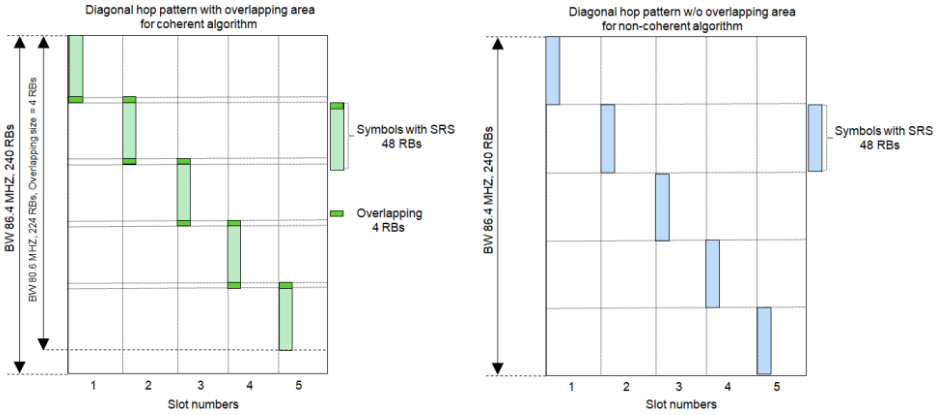


Figure 1. Illustration of a diagonal hop pattern with and without subcarriers overlapping of sounding reference signals (SRSs) from the adjacent frequency bands

It is interesting to compare the typical observation and processing duration (several slots) with the channel coherence time value, which characterize channel variations. For the considered channel model, typical coherence time is reverse proportional to the Doppler frequency spread f_d . For the LOS-dominant channel, (which is the case here), the main LOS ray will change its phase to the opposite ($\pm \pi$) over a period which is also reverse proportional to the f_d . Taking maximum speed of 120 km/h and 3.5 GHz carrier frequency, Doppler frequency (shift) will be around 390 Hz. This corresponds to the channel coherence time of 1ms – or about two slots. In our case the observation time (5 slots) is much larger than this period, and on the first glance, that may lead to the serious degradation of the ToA estimate accuracy. However, it should be noted, that the proposed coherent algorithm executes the tracking of the dominant LOS channel ray phase (it is possible due to the overlapping of neighboring slots) and therefore may improve the accuracy of the ToA estimate for some specific configurations of subcarriers overlapping and mobility parameters. Actual simulation results provided in the next sections will demonstrate all these effects in details.

4. Simulation results

In this section, we present the simulation results obtained using the developed SLS positioning. The first results of the study are focused on the question of finding the optimal overlap size required to equalize the phases for using the coherent algorithm.

On the one hand, as the overlapping bandwidth increases, the accuracy will increase due to an increase in the efficiency of phase error compensation; but on the other hand, the positioning accuracy will decrease due to a decrease in the total sounding reference signals (SRSs) frequency bandwidth.

Figure 2 shows a plot of the full set of simulation results summarizing the performance for various overlapping sizes for 5 hops for super-resolution MUSIC TDoA estimation algorithm. The curves show the 90% cumulative distribution function (CDF) values of positioning errors in meters vs. overlapping size of the adjacent SRSs, measured in the number of resource blocks (RBs). As can be seen, positioning accuracy can be significantly improved if the phase between each hop is correctly adjusted. In the case of low UE mobility (3 km/h), the overlapping of only 2 RBs (24 subcarriers) is the most optimal, phase error estimation between each pair hops already has high accuracy and a further increase in the overlapping size only results in a loss of the total band and decreases the positioning accuracy. With the growth of UE mobility, a larger overlapping size is required, so for a velocity = 120 km/h, an overlapping of 5 RBs (60 subcarriers) is optimal.

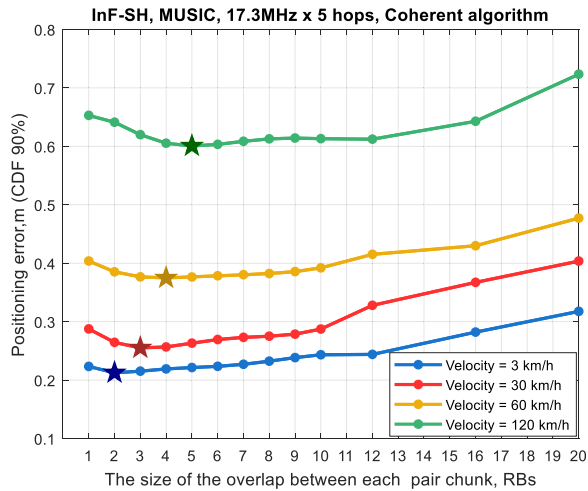


Figure 2. Plot of 90% CDF values of positioning accuracy vs. overlapping size of sounding reference signals (SRSs) from the adjacent frequency bands

Figure 3 shows the plot of the set of simulation results summarizing the effectiveness of the coherent/non-coherent algorithms for different mobility scenarios for super-resolution MUSIC TDoA estimation algorithm. This plot shows CDF values of positioning accuracy. For a coherent algorithm, a fixed overlap size equal to 4 RBs (48 subcarriers) is considered for all cases of user mobility. As can be seen, the performance of the coherent algorithm is highly dependent on the mobility of the user, since it degrades the accuracy of the phase error estimate between each hop. Thus, as the velocity of UE increases to 120 km/h, the positioning accuracy degrades by 38 cm at the CDF level of 90% (blue and green dashed curve, respectively), while the proposed non-coherent algorithm does not require phase alignment and has a very weak dependence on the mobility of the UE and loses only 3 cm at the CDF level of 90% (blue and green solid curve, respectively). The performance of the coherent algorithm is higher compared to the non-coherent algorithm for UE velocity up to 30

km/h, but after that the coherent algorithm begins to lose significantly to the non-coherent algorithm.

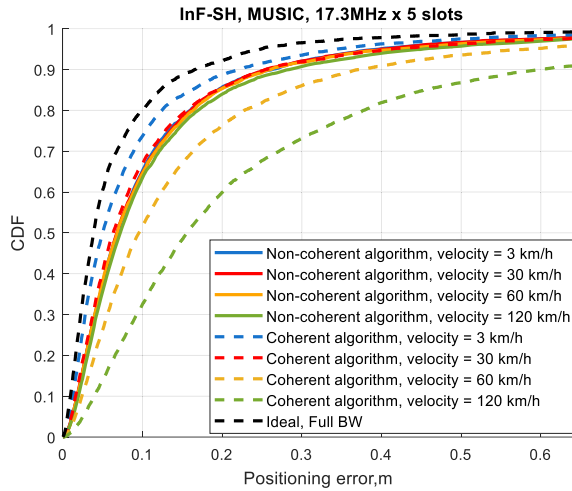


Figure 3. Performance of coherent/non-coherent algorithms of joint processing of hops

5. Summary

In this paper, we presented a detailed UE positioning performance analysis of the frequency hopping method for various mobility scenarios using the super-resolution MUSIC TDoA estimation algorithm. This analysis was carried out on the basis of the results obtained from the developed SLS simulator. It is shown that the correct operation of the coherent algorithm requires compensation of phase errors between each pair of signal frequency hops. The optimal frequency hop overlap size for phase adjustment was also found for different UE mobility cases. It is demonstrated that the proposed algorithm of non-coherent signal processing does not require signal phase correction and demonstrates its advantages for users with high mobility compared to the coherent algorithm. It follows from this that the proposed non-coherent algorithm for joint processing of frequency hops for UE with limited bandwidth can be applied in practice along with the coherent algorithm. For high mobility case it has higher performance and also does not require additional computational and overhead resources.

References

- [1] 3GPP. TR 21.916; Release 16 Description; June 2022. Version 16.2.0.
- [2] 3GPP. TR 121.917; Release 17 Description; January 2023. Version 17.0.
- [3] F. Mogyorósi et al. Positioning in 5G and 6G Networks. In: Sensors World Forum (SensorForum-2022), no. 13: 4757, June 2022. DOI: [10.3390/s22134757](https://doi.org/10.3390/s22134757).
- [4] T. K. Geok et al. Review of Indoor Positioning: Radio Wave Technology. In: Applied Sciences 11, no.1: 279, December 2020. DOI: [10.3390/app11010279](https://doi.org/10.3390/app11010279).
- [5] H. Dun, C. C. J. M. Tiberius and G. J. M. Janssen. Positioning in a Multipath Channel Using OFDM Signals with Carrier Phase Tracking. In: IEEE Access, vol. 8, pp. 13011-13028, January 2020. DOI: [10.1109/ACCESS.2020.2966070](https://doi.org/10.1109/ACCESS.2020.2966070).

- [6] L. Zhou, G. Li, Z. Zheng and X. Yang. TOA Estimation with Cross Correlation-Based MUSIC Algorithm for Wireless Location. In: 2014 Fourth International Conference on Communication Systems and Network Technologies, pp. 862-865, 2014. DOI: 10.1109/CSNT.2014.179.
- [7] Xinrong Li and Kaveh Pahlavan. Super-resolution TOA estimation with diversity for indoor geolocation. In: IEEE Transactions on Wireless Communications., vol.3, no.1, pp. 224-234, Jan. 2004. DOI: 10.1109/TWC.2003.819035.
- [8] G. M. Roshan Indika Godaliyadda and Hari K. Garg. Analysis of super resolution Spectral Estimation Techniques for indoor positioning applications. In: 9th International Conference on Signal Processing, pp. 2538-2531, October 2008. DOI: 10.1109/ICOSP.2008.4697666.
- [9] Zheng Wu, Tonghui Yang , Jinhua Wang , Xiaomei Yang , Hengzhi Cui, Xuefeng Zhai, Qingqiang Xu. Research on Motion Pattern Classification and Wavelet Denoising Based on TDOA Chan Algorithm. In: IEEE 2nd International Conference on Electronics and Communication Engineering (ICECE), pp. 66-70, December 2019. DOI: 10.1109/ICECE48499.2019.9058570.
- [10] Yanru Zhong, Ting Wang, Yining Liu, Xiaonan Luo. Indoor UWB Location Based On Residual Weighted Chan Algorithm. In: 7th International Conference on Digital Home (ICDH), pp. 274-279, February 2019. DOI: 10.1109/ICDH.2018.00055.
- [11] Zhang Jian-wu, Yu Cheng-lei, Tang Bin, Ji Ying-ying. Chan Location Algorithm Application in 3-Dimension Space Location. In: ISECS International Colloquium on Computing, Communication, Control, and Management, pp. 622-625. August 2008. DOI: 10.1109/CCCM.2008.76.
- [12] Ziad Hatab, Hiroaki Takahashi, Michael Gadringer. OFDM Symbol-timing and Carrier-frequency Offset Estimation Based on Singular Value Decomposition. In: International Conference on Broadband Communications for Next Generation Networks and Multimedia Applications (CoBCom), July 2022. DOI: 10.1109/CoBCom55489.2022.9880699.
- [13] Dinh Van Linh, Vu Van Yem. Carrier Frequency Offset Estimation and Compensation Technique for Massive MIMO-OFDM Wireless Communication System. July 2022. DOI: 10.1109/ICECET55527.2022.9872995.
- [14] Hongbao Zhang. A Joint Scheme for Carrier Frequency Offset Estimation, Carrier Phase Correction and Timing. In: 3rd International Conference on Electrical Engineering and Control Technologies (CEECT), December 2021. DOI: 10.1109/CEECT198.2021.9672646.
- [15] 3GPP. TS 38.901 NR; Study on channel model for frequencies from 0.5 to 100 GHz; April 2022. Version 17.1.0 Release 17.
- [16] 3GPP. TS 38.211 NR; Physical channels and modulation; September 2023. Version 17.6.0 Release 17.